



Geophysical Research Letters

RESEARCH LETTER

10.1029/2019GL085748

Key Points:

- Lightning proxies are studied in cloud-resolving simulations of global warming over the United States and the tropical ocean
- All the proxies predict that lightning increases over the United States in the range of 8–16% per kelvin
- The proxies disagree over the tropical ocean, predicting either a substantial increase of 5–12%/K or a moderate decrease of 1–4%/K

Supporting Information:

- Supporting Information S1

Correspondence to:

D. M. Romps,
romps@berkeley.edu

Citation:

Romps, D. M. (2019). Evaluating the future of lightning in cloud-resolving models. *Geophysical Research Letters*, 46, 14,863–14,871. <https://doi.org/10.1029/2019GL085748>

Received 8 OCT 2019

Accepted 29 NOV 2019

Accepted article online 3 DEC 2019

Published online 23 DEC 2019

Evaluating the Future of Lightning in Cloud-Resolving Models

David M. Romps^{1,2}

¹Department of Earth and Planetary Science, University of California, Berkeley, CA, USA, ²Climate and Ecosystem Sciences Division, Lawrence Berkeley National Laboratory, Berkeley, CA, USA

Abstract Two proxies for lightning predict very different responses to global warming: the CAPE times precipitation proxy predicts a large increase in lightning over both the continental United States and the tropical oceans, while the ice flux proxy predicts a small increase over the United States and a decrease over the tropical oceans. To date, however, these proxies have been studied only in global climate models with parameterized convection. Here, cloud-resolving simulations are used to assess their predictions of future lightning rates. Over the United States, all proxies predict a large increase in the lightning rate in the range of 8–16%/K. On the other hand, in the tropics as modeled by radiative convective equilibrium, half of the proxies predict an increase (of 5–12%/K), while the other half predict a decrease (of 1–4%/K). The reasons for the different responses of these proxies is explored, but it remains unclear which proxy is best suited to predicting future lightning rates.

1. Introduction

In recent years, two meteorological proxies for lightning have been proposed: the product of convective available potential energy (CAPE) times the precipitation rate P (Romps et al., 2014) and the midtropospheric convective flux of ice (Finney et al., 2014). The CAPE $\times P$ proxy has been shown to be a good match to observations (Romps et al., 2014, 2018; Tippet et al., 2019) as has the ice flux proxy (Finney et al., 2014, 2016). But it appears that these proxies make very different predictions for the impact of global warming on lightning strike rates. Over the continental United States (CONUS), the CAPE $\times P$ proxy predicts a $12 \pm 5\%$ increase in CONUS lightning strike rate per kelvin of global-mean temperature increase (Romps et al., 2014), while the ice flux proxy predicts an increase over CONUS of only 3.4%/K.

For the tropics, the predictions are even more divergent. Because tropical CAPE is expected to increase by about 8%/K (Romps, 2014, 2016; Seeley & Romps, 2015) and tropical precipitation is expected to increase by about 2%/K (Held & Soden, 2006; Jeevanjee & Romps, 2018; Lambert & Webb, 2008; Stephens & Ellis, 2008), we expect tropical CAPE $\times P$ and, therefore, tropical lightning to increase at about 10% per K of local surface-air temperature change. But the simulations of Finney et al. (2018) found a 5%/K decrease in tropical lightning. (Finney et al. (2018) report in their Table S1 a 28.3% decline in the tropical flash rate from a global-mean temperature change given in their Figure S2 as 4.87 K. From these, we can calculate $\log(1.283)/4.87 = 0.05/\text{K}$.)

To date, these proxies have been evaluated only in global climate models (GCMs) with parameterized convection. Here, we take advantage of two preexisting cloud-resolving simulations of global warming in an attempt to (1) evaluate the performance of these and other lightning proxies over CONUS in today's climate, (2) assess whether the CONUS lightning flash rate will increase at O(10)%/K or just a few %/K, and (3) ascertain whether lightning over the tropical oceans should increase or decrease with warming.

2. Simulations

The analysis presented here will take advantage of two sets of simulations available from other studies: a pair of 13-year-long cloud-resolving simulations over CONUS (RM. Rasmussen & Liu, 2017) and three 4-year-long cloud-resolving simulations of tropical radiative convective equilibrium (RCE) over a slab ocean.

2.1. WRF Simulations of CONUS

The pair of cloud-resolving simulations over CONUS were conducted with the Weather Research and Forecasting (WRF) model v3.4.1 using a 4-km horizontal grid spacing (RM. Rasmussen & Liu, 2017).

The simulations used the Thompson aerosol-aware, six-class, bulk microphysics scheme (G. Thompson & Eidhammer, 2014) and the Rapid Radiative Transfer Model for General Circulation Models (RRTMG; Clough et al., 2005; Iacono et al., 2008). The first simulation was a control (CTRL) simulation covering 13 years from October 2000 to September 2013, and data are analyzed here over the 7-year period from 1 January 2006 to 31 December 2012. To reproduce the broad outlines of the actual weather, the model's temperature, geopotential height, and wind were nudged on large scales to the ERA-Interim reanalysis (Dee et al., 2011; Liu et al., 2017; KL. Rasmussen et al., 2017). The second simulation is a pseudo global warming (PGW) simulation that was identical to CTRL except that the nudging targets were set equal to ERA-Interim plus the model-ensemble-mean changes in monthly climatology over the 21st century (mean over 2071–2100 minus mean over 1976–2005) from the CMIP5 simulations of the RCP8.5 scenario. This modeling approach captures the effect of global warming on thermodynamic fields but does not capture possible changes to the large-scale circulation, such as a shift in the storm track. For both CTRL and PGW, lightning proxies are calculated here using the three-dimensional snapshots that were saved every three hours.

2.2. DAM Simulations of RCE

The three cloud-resolving simulations of tropical, maritime RCE were conducted with Das Atmosphärische Modell (DAM; Romps, 2008) using a 1-km horizontal grid spacing on a 108-km-wide square domain. The simulations used a six-class, single-mode, bulk microphysics scheme (Krueger et al., 1995; Lin et al., 1983; Lord et al., 1984) and RRTMG (Clough et al., 2005; Iacono et al., 2008). The three simulations were identical except for the concentrations of carbon dioxide, which were set to 280, 1,120 (i.e., 4 \times), and 4,480 ppmv (i.e., 16 \times). By definition, RCE does not have any large-scale circulation that could export energy out of the column, so a cooling of 112 W/m² was applied to the slab ocean to guarantee that the 280-ppmv simulation equilibrated to a sea surface temperature (SST) of 300 K (to give values of CO₂ and SST that are representative of the preindustrial tropics). The 4 \times and 16 \times simulations equilibrated to an SST of 306 and 315 K, respectively. In this study, lightning proxies are calculated at every time step during a 100-day simulation that was restarted from the end of the 4-year equilibration period.

3. Proxies

With these cloud-resolving models, we will look at the behavior of four lightning proxies: two proxies based on storm intensity and precipitation rate (CAPE \times P and PW10) and two proxies based on the properties of ice in storm clouds (IFluxT and I \times G).

3.1. CAPE \times P

CAPE \times P was introduced by Romps et al. (2014) and has been validated extensively over CONUS (Romps et al., 2014, 2018; Tippett et al., 2019). In the cloud-resolving simulations over CONUS used in section 4, CAPE is calculated instantaneously, the precipitation rate P is averaged over the ensuing three hours, and CAPE \times P is defined as their product. In the cloud-resolving simulations of RCE used in section 5, CAPE is calculated from mean profiles and P is taken to be the mean precipitation rate.

3.2. PW10

A closely related proxy, which we define here and denote by PW10, is the precipitation rate conditioned on there being a vertical velocity exceeding 10 m/s in the column above. This proxy is motivated by evidence that a sufficiently high vertical velocity, of around 10 m/s, is needed to generate lightning (E. Zipser & Lutz, 1994; E.J. Zipser, 1994). We might expect PW10 to behave similarly to CAPE \times P since higher CAPE will tend to generate more updrafts with vertical velocities exceeding 10 m/s. Unlike CAPE \times P, however, it is typically not possible to calculate PW10 from reanalysis or GCMs since the relevant convective velocities are not resolved.

3.3. IFluxT

In their study of future lightning rates, Finney et al. (2018) used a proxy that has been referred to as IFLUX (Finney et al., 2014) and ICEFLUX (Finney et al., 2016) and is defined as the vertical flux of ice mass at a pressure of 44 kPa. Let us refer to this proxy as IFluxP, with a P to denote the fact that this is evaluated on a surface of constant pressure. We calculate it here as the upward mass flux of cloud ice on the 44-kPa surface where the vertical velocity exceeds 1 m/s. Both WRF and DAM use a bulk microphysics scheme with six classes (vapor, cloud water, cloud ice, rain, snow, and graupel) and only the ice class is used in this calculation (i.e., "QICE" in WRF and "qi" in DAM). The vertical-velocity restriction focuses the proxy

on convective updrafts and should exclude, for example, cirrus clouds that are gently oscillating due to gravity waves.

As shown in supporting information Figure S1, the IFluxP proxy greatly exaggerates the lightning over the mountainous Western United States in all but the summer months. Another problem with the IFluxP proxy is that its definition on a fixed isobar makes it poorly suited to the study of global warming. To see why, note that lightning is caused by charging that takes place in the mixed-phase region of clouds (Williams et al., 1991), and the mixed-phase cloud region is bounded by the 273-K isotherm (where ice can first form) and the 240-K isotherm (where liquid drops freeze homogeneously). Therefore, the charging layer will follow the isotherms with global warming, not the isobars. In addition, many related properties of the atmosphere have also been shown to follow isotherms much more closely than isobars, for example, relative humidity (Romps, 2014), cloud anvils (Hartmann & Larson, 2002), the tropopause (DWJ. Thompson et al., 2017; Seeley et al., 2019), and radiative cooling (Jeevanjee & Romps, 2018). Therefore, we use here IFluxT, defined to be the convective ice flux on the 260-K isotherm, which lies within the mixed-phase regions of clouds and is close to the 440-mbar isobar in a modern-day tropical sounding. As shown in Figure S1, the use of IFluxT instead of IFluxP eliminates the spurious values over the Western US.

3.4. I × G

Laboratory experiments show that electrification is generated by the collision of ice particles with riming graupel in the mixed-phase region of a cloud (Takahashi, 1978). All else equal, the rate of collisions between ice and graupel, and so the rate of electrification, will be proportional to the product of their respective number concentrations. The phrase “all else equal” is a significant leap of faith here since the “all else” includes size distributions, free-fall speeds, and riming rates, but it is no more a leap of faith than is required for the other lightning proxies. In this spirit, let us define the I × G lightning proxy as the vertical integral of the product of the densities of ice and graupel.

In summary, the four proxies are defined as

$$\text{“CAPE} \times \text{P”}(x, y, t) = \text{CAPE}(x, y, t)P(x, y, t) \quad (1)$$

$$\text{“PW10”}(x, y, t) = P(x, y, t)\mathcal{H}\left(\max_z w(x, y, z, t) - 10 \text{ m/s}\right) \quad (2)$$

$$\text{“IFluxT”}(x, y, t) = \rho_i(x, y, z', t)w(x, y, z', t)\mathcal{H}\left[w(x, y, z', t) - 1 \text{ m/s}\right] \quad (3)$$

where $T(x, y, z') = 260 \text{ K}$

$$\text{“I} \times \text{G”}(x, y, t) = \int_0^\infty dz \rho_i(x, y, z, t)\rho_g(x, y, z, t), \quad (4)$$

where CAPE (J/kg) is the convective available potential energy calculated for isentropic ascent of near-surface air, P ($\text{kg}\cdot\text{m}^{-2}\cdot\text{s}^{-1}$) is the precipitation rate, \mathcal{H} is the Heaviside unit step function, w (m/s) is the vertical velocity, ρ_i (kg/m^3) is the mass of ice per volume of air, ρ_g (kg/m^3) is the mass of graupel per volume of air, and T (K) is the air temperature.

4. CONUS Lightning

Using the cloud-resolving WRF simulations over CONUS, we can address the first two questions from section 1: whether these four proxies are reliable in today’s climate and whether they predict a small (few %/K) or large ($\sim 10\%/K$) increase in CONUS lightning with global warming.

4.1. Proxy Validation Over CONUS

To evaluate these proxies in today’s climate, we can use the monthly mean maps of lightning flash rates over CONUS from the National Lightning Detection Network (NLDN; Orville & Huffines, 2001; Wacker & Orville, 1999). Figure 1 shows scatterplots of the horizontally averaged monthly climatology of each proxy in the WRF CTRL simulation (averaged over 2006 to 2012) against the horizontally averaged monthly climatology of NLDN lightning strike rate (averaged over 2006 to 2012) for each of four quadrants of CONUS defined by boundaries at 99°W and 39°N . Despite biases in the WRF simulation (e.g., low biases in CAPE and precipitation in the Central United States, not shown here), we see that all of the proxies perform well in comparison to the monthly climatology of observed lightning strikes, with R^2 values of 0.75 and higher.

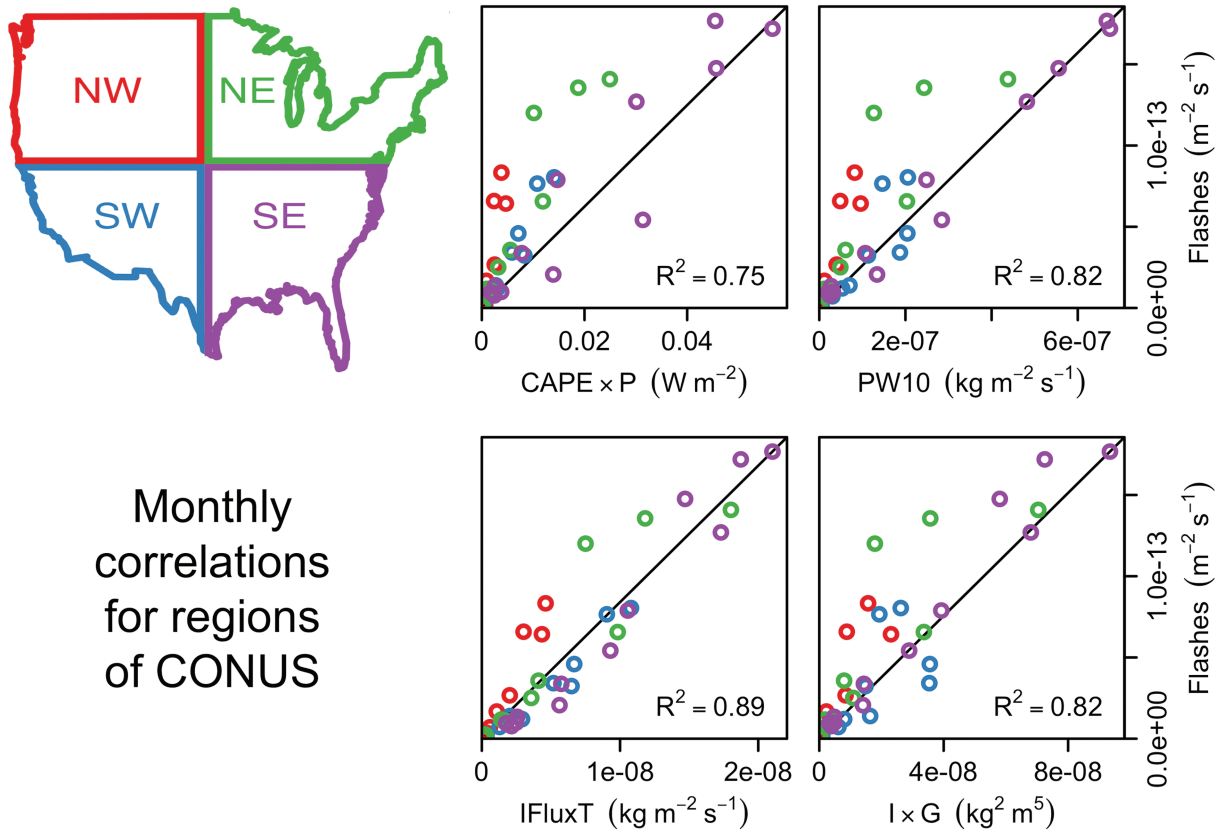


Figure 1. Monthly climatology of flash rate per area versus proxy for each of the four proxies (the four panels) and each of the four regions of CONUS (the four colors within each scatterplot) calculated with WRF and NLDN data from 2006 through 2012. Each scatterplot has $4 \times 12 = 48$ points corresponding to a monthly climatology for each of the four regions.

WRF’s biases in CAPE and precipitation are a particular hindrance to the performance of $\text{CAPE} \times P$ here. When the calculation is repeated using $\text{CAPE} \times P$ from the National Centers for Environmental Prediction (NCEP) North American Regional Reanalysis (NARR; Mesinger et al., 2006) the R^2 jumps to 0.86; see Figure S2.

4.2. CONUS Projections

The global-warming-induced increase in annual-mean, CONUS-mean proxy values can be expressed as a fractional change per degree of mean warming according to

$$\text{Fractional change in } X \text{ per K of warming} = \frac{\log(\bar{X}_2) - \log(\bar{X}_1)}{\bar{T}_2 - \bar{T}_1}, \quad (5)$$

where the overbar is a horizontal and temporal average, T is the near-surface air temperature, and subscripts 1 and 2 correspond to the CTRL and PGW simulations, respectively. The fractional changes in the proxies over CONUS are shown in Figure 2a. We see that $\text{CAPE} \times P$, PW10, IFluxT, and $I \times G$ all increase with warming; they increase at rates of 9%/K, 16%/K, 8%/K, and 13%/K, respectively. The 9% per K of local warming found here for $\text{CAPE} \times P$ here is consistent with the 12% per K of global warming obtained by Romps et al. (2014) once we account for the 50% enhancement of land warming over ocean warming (Sutton et al., 2007), which translates into a 30% enhancement of land warming over the warming of the global mean: note that $1.3 \times 9 \approx 12$. Therefore, we conclude that all proxies, including IFluxT, predict an increase in lightning over CONUS at the rate of $O(10)\%/K$. In particular, the 8%/K increase predicted by IFluxT in this cloud-resolving model is more than twice the increase of 3.4%/K predicted by Finney et al. (2018) using IFluxP in a GCM with parameterized convection.

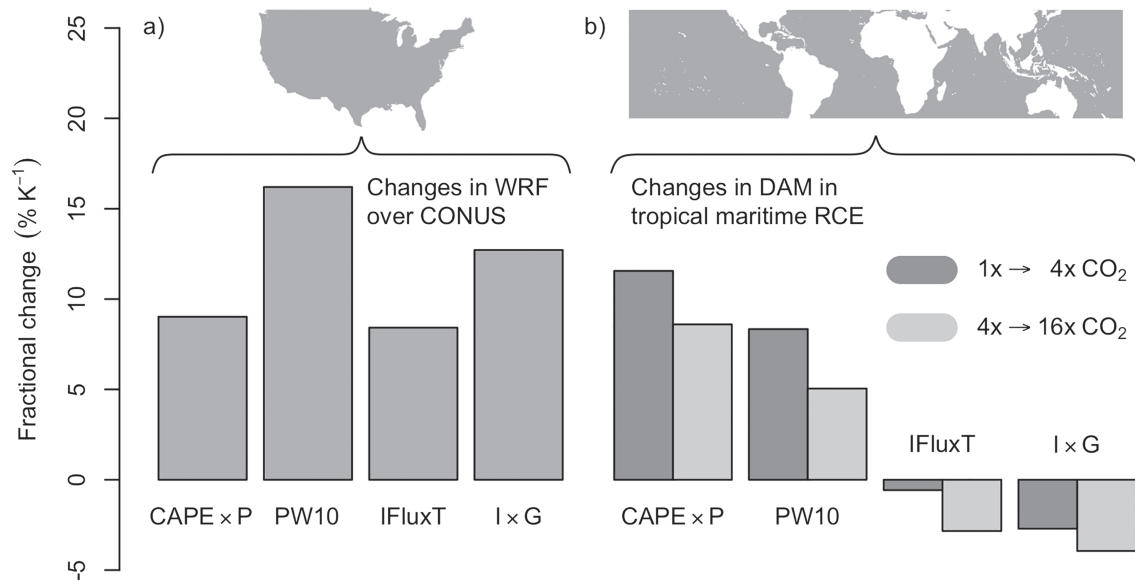


Figure 2. (a) From CTRL to PGW in the simulations over CONUS, the increase in the annual-mean CONUS-mean lightning proxies expressed as a fractional change per degree of annual-mean CONUS-mean surface-air temperature change. (b) From 1× to 4×CO₂ (dark gray) and 4× to 16×CO₂ (light gray) in the slab ocean simulations of tropical, maritime RCE, the fractional change in proxies per degree of SST change.

5. Tropical Lightning

Using the cloud-resolving DAM simulations of RCE over a slab ocean, we can attempt to address the third question from section 1: whether global warming will cause tropical maritime lightning rates to increase or decrease.

5.1. Tropical Projections

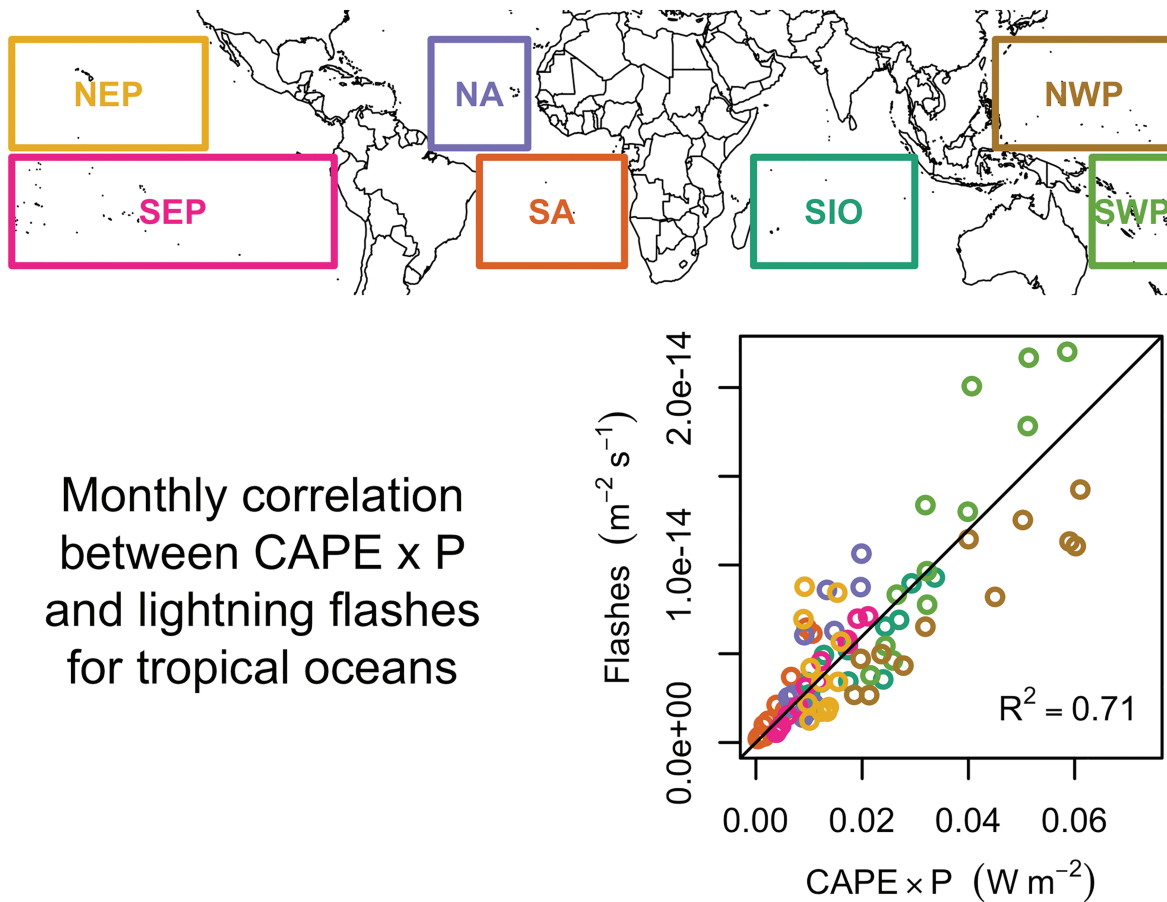
To examine the predictions of the lightning proxies in a tropical atmosphere, we calculate the mean values of the proxies in each of three slab ocean simulations (with 1×, 4×, and 16× the preindustrial concentration of CO₂). Fractional changes per degree of SST warming are calculated as in equation (5) with T representing the slab ocean temperature and subscripts 1 and 2 corresponding to slab ocean simulations with different atmospheric CO₂ concentrations. Figure 2b shows the fractional increases in the four proxies between the 1× and 4× simulations (dark gray bars) and between the 4× and 16× simulations (light gray bars). We see that the proxies do not agree on the sign of the change: CAPE × P and PW10 predict increases of 9–12%/K and 5–8%/K, respectively, but IFluxT and I × G predict decreases of 1–3%/K and 3–4%/K, respectively. Consistent with expectations, the increases in CAPE × P are driven by increases in CAPE of 7–9%/K and increases in P of 1–3%/K.

Even though IFluxT is predicting a decrease in lightning, the decrease is at a rate of 1–3%/K, which is smaller than the 5%/K decline for the tropics predicted by the GCM modeling of Finney et al. (2018). This difference may be due, in part, to the fact that the latter result is for the entire tropics, including both ocean and land. Nevertheless, these RCE simulations confirm, within a cloud-resolving model, that the CAPE × P and IFluxT proxies make very different predictions for the future of maritime tropical lightning.

5.2. Proxy Validation in the Tropics

One possible explanation for the discrepancy between CAPE × P and IFluxT is that CAPE × P simply does not work in the tropics. To check this, we can compare tropical oceanic CAPE × P calculated from reanalysis with tropical oceanic lightning measured by the World Wide Lightning Location Network (WWLLN; Hutchins et al., 2012; Jacobson et al., 2006; Virts et al., 2013). The reason for focusing on the oceans here is twofold: (1) for consistency with the RCE simulations and (2) because an analysis of both land and ocean would run afoul of the fact that both CAPE × P and IFluxP greatly underestimate the land/ocean lightning contrast (Finney et al., 2014; Roms et al., 2018).

For this analysis, we will look at the monthly climatology of CAPE × P and lightning in the seven tropical ocean basins demarcated at the top of Figure 3. The European Centre for Medium-Range Weather Forecasts



Monthly correlation
between CAPE \times P
and lightning flashes
for tropical oceans

Figure 3. Monthly climatology of observed flash rate per area versus the monthly climatology of reanalysis CAPE \times P for each of seven ocean basins (the seven colors in the scatterplot). The scatterplot has $7 \times 12 = 84$ points corresponding to a monthly climatology for each of the seven ocean basins.

(ECMWF) reanalysis, referred to as ERA-Interim (ERA; Dee et al., 2011), is used to calculate 3-hourly global maps of CAPE \times P over 11 years (from 2005 to 2015, inclusive). These are then averaged to give a monthly climatological value within each of these basins. Plotting the $7 \times 12 = 84$ monthly per-basin WWLLN flash rate densities against the corresponding 84 ECMWF CAPE \times P values, we get the scatterplot in Figure 3. We see that CAPE \times P does a very good job of capturing the month-to-month and interbasin variations in tropical lightning. (Note that both the flash rate and CAPE \times P are expressed as rates per area so that differences in basin size are not contributing to the correlation here.) The fact that this correlation is so strong is all the more remarkable given that reanalyses are poorly constrained by observations over the oceans. We conclude, therefore, that CAPE \times P cannot be discarded as a tropical maritime lightning proxy based on a comparison with the current climatology. Finney et al. (2016) subjected the IFluxP proxy to a related test and found that it also performed well in this regard. So, we are left with two proxies that both perform reasonably well in today's climate but which predict very different responses of tropical lightning to global warming.

6. Discussion

To help understand how IFluxT and $I \times G$ could decrease at the same time that CAPE \times P and PW10 increase, Figure 4 plots some relevant vertical profiles from the three slab ocean simulations, color-coded as blue, black, and red for the $1\times$, $4\times$, and $16\times\text{CO}_2$ simulations, respectively. We know that global warming increases CAPE (Romps, 2014, 2016; Seeley & Romps, 2015; Singh & O'Gorman, 2013), and higher CAPE should give updrafts a higher buoyancy. This is confirmed by Figure 4a, which plots the mass-flux-weighted mean buoyancy of updrafts, defined as regions with $w > 1$ m/s, plotted against temperature as a height variable. We see that the buoyancy of updrafts increases with warming, consistent with the increase in CAPE. A natural consequence of higher buoyancy is a higher vertical velocity, and this plays out as expected, as seen in Figure 4b.

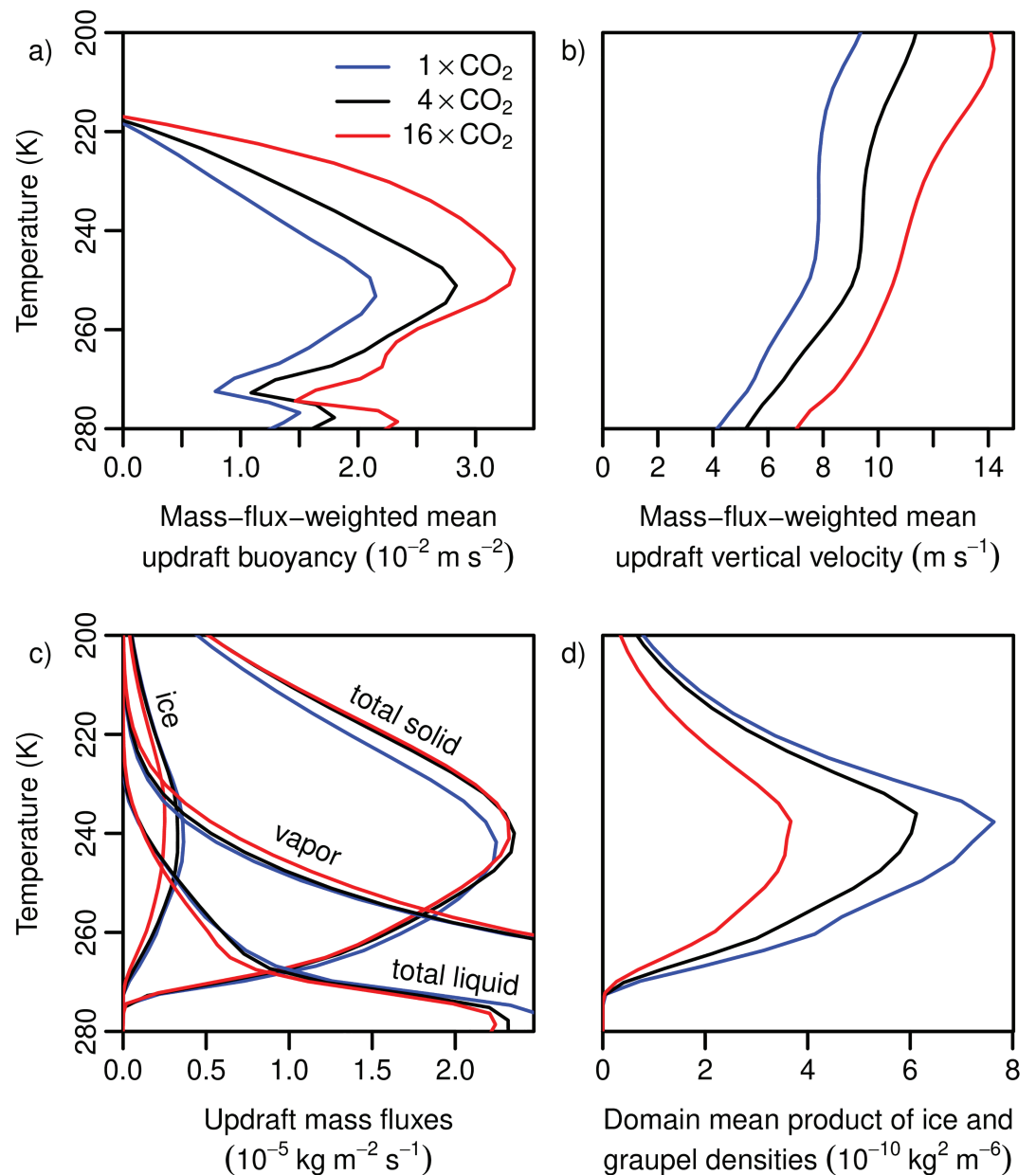


Figure 4. For the (blue) 1×, (black) 4×, and (red) 16×CO₂ tropical RCE simulations, mean profiles, plotted against temperature as a height coordinate, of (a) mass-flux-weighted updraft buoyancy, (b) mass-flux-weighted updraft vertical velocity, (c) updraft mass fluxes of various categories of water, and (d) domain mean product of the densities of ice and graupel.

Although convective vertical velocities increase with warming, Figure 4c shows that the mass fluxes of various water substances are roughly invariant functions of isotherm. Here, the mass flux of total liquid is calculated as the horizontal and temporal average of $(\rho_c + \rho_r)w\mathcal{H}(w - 1 \text{ m/s})$, where ρ_c and ρ_r are the densities of cloud liquid and rain. (Note that rain falls relative to the dry air, so this is not the *net* flux of liquid water in updrafts.) Similarly, the mass flux of total solid is calculated as $(\rho_i + \rho_s + \rho_g)w\mathcal{H}(w - 1 \text{ m/s})$, where ρ_i , ρ_s , and ρ_g are the densities of cloud ice, snow, and graupel, respectively.

The invariance of these mass fluxes is remarkable, but not entirely unexpected. Recent work has demonstrated that, in RCE, both relative humidity and radiative cooling rates are approximately invariant functions of temperature (Jeevanjee & Romps, 2018; Romps, 2014). To the extent that net radiative cooling above a given isotherm is balanced by the vertical eddy flux of latent enthalpy at that isotherm, the invariance of

that net radiative cooling (Jeevanjee & Romps, 2018) implies that $Mq_v^*(1 - RH)$, where M is the convective mass flux and q_v^* is the saturation mass fraction, is an invariant function of isotherm. Since RH is also an invariant function of isotherm (Romps, 2014), we conclude that the water vapor mass flux Mq_v^* must be an invariant function of isotherm. Indeed, we see that this prediction is borne out to good approximation in Figure 4c. It is harder to explain the concomitant invariance of the mass fluxes of condensates, but note that these condensates ultimately derive from the condensation of water vapor, which is directly related to the vertical gradient of $Mq_v^*(1 - RH)$, which is temperature-invariant. And, while Figure 4c shows that the water mass fluxes are approximately conserved, there are some variations on fixed isotherms from one simulation to the next. For ice, whose mass flux is a small fraction of the total solid mass flux, those small variations produce the small fractional changes of IFluxT in Figure 2b.

While the IFluxT proxy is a measure of the flux of ice, the $I \times G$ proxy is a measure of the stock of ice and graupel. In Figure 4d, we see that the domain mean product of ice and graupel densities—that is, $\rho_i \rho_g$ —experiences much bigger fractional changes with warming. We note that this would be expected even if the mass fluxes were exact functions of isotherm, and we would expect this because of the higher CAPE. Higher CAPE leads to greater updraft buoyancy, which leads to higher vertical velocities (as seen in panels a and b). Those higher vertical velocities imply that an invariant water mass flux must be occurring over a smaller fractional area. Or, in other words, by having the same ice flux at a higher vertical velocity, the presence of condensates in updrafts is more fleeting, and so $I \times G$ is smaller; as shown in Figure S3, the domain mean densities of both ice and graupel decrease with warming.

In summary, we can understand the different responses of the four proxies in tropical, maritime RCE in the following way. We expect small changes in water mass fluxes since they are approximately described as fixed functions of isotherm (thus, the IFluxT proxy predicts very little change in tropical lightning). At the same time, we expect much higher CAPE and higher updraft velocities (thus, CAPE \times P and PW10 predict large increases in tropical lightning). However, those higher vertical velocities lead to a decrease in the column-integrated stock of cloud ice (thus, $I \times G$ predicts a marked decrease in tropical lightning). But it remains to be seen which of these proxies, if any, is accurately forecasting the future of tropical lightning in a warmer world.

Acknowledgments

This work was supported by the Laboratory Directed Research and Development Program of Lawrence Berkeley National Laboratory under the U.S. Department of Energy Contract DE-AC02-05CH11231. Data analysis was performed on the Lawrence computational cluster resource provided by the IT Division at the Lawrence Berkeley National Laboratory. Data from the WRF simulations are available online (at <https://doi.org/10.5065/D6V40SXP>).

References

- Clough, S. A., Shephard, M. W., Mlawer, E. J., Delamere, J. S., Iacono, M. J., Cady-Pereira, K., et al. (2005). Atmospheric radiative transfer modeling: a summary of the AER codes. *Journal of Quantitative Spectroscopy and Radiative Transfer*, 91(2), 233–244. <https://doi.org/10.1016/j.jqsrt.2004.05.058>
- Dee, D. P., Uppala, S. M., Simmons, A. J., Berrisford, P., Poli, P., Kobayashi, S., et al. (2011). The ERA-Interim reanalysis: Configuration and performance of the data assimilation system. *Quarterly Journal of the Royal Meteorological Society*, 137(656), 553–597. <https://doi.org/10.1002/qj.828>
- Finney, D. L., Doherty, R. M., Wild, O., & Abraham, N. L. (2016). The impact of lightning on tropospheric ozone chemistry using a new global lightning parametrization. *Atmospheric Chemistry and Physics*, 16(12), 7507–7522. <https://doi.org/10.5194/acp-16-7507-2016>
- Finney, D. L., Doherty, R. M., Wild, O., Huntrieser, H., Pumphrey, H. C., & Blyth, A. M. (2014). Using cloud ice flux to parametrise large-scale lightning. *Atmospheric Chemistry and Physics*, 14(23), 12,665–12,682. <https://doi.org/10.5194/acp-14-12665-2014>
- Finney, D. L., Doherty, R. M., Wild, O., Stevenson, D. S., MacKenzie, I. A., & Blyth, A. M. (2018). A projected decrease in lightning under climate change. *Nature Climate Change*, 8(3), 210–213. <https://doi.org/10.1038/s41558-018-0072-6>
- Hartmann, D., & Larson, K. (2002). An important constraint on tropical cloud-climate feedback. *Geophysical Research Letters*, 29(20), 1951. <https://doi.org/10.1029/2002GL015835>
- Held, I. M., & Soden, B. J. (2006). Robust responses of the hydrological cycle to global warming. *Journal of Climate*, 19(21), 5686–5699. <https://doi.org/10.1175/JCLI3990.1>
- Hutchins, M. L., Holzworth, R. H., Brundell, J. B., & Rodger, C. J. (2012). Relative detection efficiency of the World Wide Lightning Location Network. *Radio Science*, 47, RS6005. <https://doi.org/10.1029/2012RS005049>
- Iacono, M. J., Delamere, J. S., Mlawer, E. J., Shephard, M. W., Clough, S. A., & Collins, W. D. (2008). Radiative forcing by long-lived greenhouse gases: Calculations with the AER radiative transfer models. *Journal of Geophysical Research*, 113, D13103. <https://doi.org/10.1029/2008JD009944>
- Jacobson, A. R., Holzworth, R., Harlin, J., Dowden, R., & Lay, E. (2006). Performance assessment of the World Wide Lightning Location Network (WWLLN), using the Los Alamos Sferic Array (LASA) as ground truth. *Journal of Atmospheric and Oceanic Technology*, 23(8), 1082–1092. <https://doi.org/10.1175/JTECH1902.1>
- Jeevanjee, N., & Romps, D. M. (2018). Mean precipitation change from a deepening troposphere. *Proceedings of the National Academy of Sciences*, 115(45), 11,465–11,470. <https://doi.org/10.1073/pnas.1720683115>
- Krueger, S., Fu, Q., Liou, K., & Chin, H. (1995). Improvements of an ice-phase microphysics parameterization for use in numerical simulations of tropical convection. *Journal of Applied Meteorology*, 34(1), 281–287. [https://doi.org/10.1175/1520-0450\(1995\)34<281:1.281](https://doi.org/10.1175/1520-0450(1995)34<281:1.281)
- Lambert, F. H., & Webb, M. J. (2008). Dependency of global mean precipitation on surface temperature. *Geophysical Research Letters*, 35, L16706. <https://doi.org/10.1029/2008GL034838>
- Lin, Y., Farley, R., & Orville, H. (1983). Bulk parameterization of the snow field in a cloud model. *Journal of Applied Meteorology*, 22(6), 1065–1092. [https://doi.org/10.1175/1520-0450\(1983\)022<1065:BPOTSF>2.0.CO;2](https://doi.org/10.1175/1520-0450(1983)022<1065:BPOTSF>2.0.CO;2)

- Liu, C., Ikeda, K., Rasmussen, R., Barlage, M., Newman, A. J., Prein, A. F., et al. (2017). Continental-scale convection-permitting modeling of the current and future climate of North America. *Climate Dynamics*, *49*(1-2), 71–95. <https://doi.org/10.1007/s00382-016-3327-9>
- Lord, S., Willoughby, H., & Piotrowicz, J. (1984). Role of a parameterized ice-phase microphysics in an axisymmetric, nonhydrostatic tropical cyclone model. *Journal of the Atmospheric Sciences*, *41*(19), 2836–2848. [https://doi.org/10.1175/1520-0469\(1984\)041<2836:ROAPIP>2.0.CO;2](https://doi.org/10.1175/1520-0469(1984)041<2836:ROAPIP>2.0.CO;2)
- Mesinger, F., DiMego, G., Kalnay, E., Mitchell, K., Shafran, P. C., Ebisuzaki, W., et al. (2006). North American regional reanalysis. *Bulletin of the American Meteorological Society*, *87*(3), 343–360. <https://doi.org/10.1175/BAMS-87-3-343>
- Orville, R. E., & Huffines, G. R. (2001). Cloud-to-ground lightning in the United States: NLDN results in the first decade, 1989–1998. *Monthly Weather Review*, *129*(5), 1179–1193. [https://doi.org/10.1175/1520-0493\(2001\)129<1179:CTGLIT>2.0.CO;2](https://doi.org/10.1175/1520-0493(2001)129<1179:CTGLIT>2.0.CO;2)
- Rasmussen, K. L., Prein, A. F., Rasmussen, R. M., Ikeda, K., & Liu, C. (2017). Changes in the convective population and thermodynamic environments in convection-permitting regional climate simulations over the United States. *Climate Dynamics*. <https://doi.org/10.1007/s00382-017-4000-7>
- Rasmussen, R. M., & Liu, C. (2017). *High resolution WRF simulations of the current and future climate of North America* (Tech. Rep.). National Center for Atmospheric Research. Research Data Archive of the Computational and Information Systems Laboratory. Boulder, CO: National Center for Atmospheric Research. <https://doi.org/10.5065/D6V40SXP>
- Romps, D. M. (2008). The dry-entropy budget of a moist atmosphere. *Journal of the Atmospheric Sciences*, *65*(12), 3779–3799. <https://doi.org/10.1175/2008JAS2679.1>
- Romps, D. M. (2014). An analytical model for tropical relative humidity. *Journal of Climate*, *27*(19), 7432–7449. <https://doi.org/10.1175/JCLI-D-14-00255.1>
- Romps, D. M. (2016). Clausius-Clapeyron scaling of CAPE from analytical solutions to RCE. *Journal of the Atmospheric Sciences*, *73*(9), 3719–3737. <https://doi.org/10.1175/JAS-D-15-0327.1>
- Romps, D. M., Charn, A. B., Holzworth, R. H., Lawrence, W. E., Molinari, J., & Vollaro, D. (2018). CAPE times P explains lightning over land but not the land-ocean contrast. *Geophysical Research Letters*, *45*, 12,623–12,630. <https://doi.org/10.1029/2018GL080267>
- Romps, D. M., Seeley, J. T., Vollaro, D., & Molinari, J. (2014). Projected increase in lightning strikes in the United States due to global warming. *Science*, *346*(6211), 851–854. <https://doi.org/10.1126/science.1259100>
- Seeley, J. T., Jeevanjee, N., & Romps, D. M. (2019). FAT or FITT: Are anvil clouds or the tropopause temperature-invariant? *Geophysical Research Letters*, *46*, 1842–1850. <https://doi.org/10.1029/2018GL080096>
- Seeley, J. T., & Romps, D. M. (2015). Why does tropical convective available potential energy (CAPE) increase with warming? *Geophysical Research Letters*, *42*, 10,429–10,437. <https://doi.org/10.1002/2015GL066199>
- Singh, M. S., & O’Gorman, P. A. (2013). Influence of entrainment on the thermal stratification in simulations of radiative-convective equilibrium. *Geophysical Research Letters*, *40*, 4398–4403. <https://doi.org/10.1002/grl.50796>
- Stephens, G., & Ellis, T. (2008). Controls of global-mean precipitation increases in global warming GCM experiments. *Journal of Climate*, *21*(23), 6141–6155. <https://doi.org/10.1175/2008JCLI2144.1>
- Sutton, R. T., Dong, B., & Gregory, J. M. (2007). Land/sea warming ratio in response to climate change: IPCC AR4 model results and comparison with observations. *Geophysical Research Letters*, *34*, L02701. <https://doi.org/10.1029/2006GL028164>
- Takahashi, T. (1978). Riming electrification as a charge generation mechanism in thunderstorms. *Journal of the Atmospheric Sciences*, *35*(8), 1536–1548. [https://doi.org/10.1175/1520-0469\(1978\)035<1536:REAACG>2.0.CO;2](https://doi.org/10.1175/1520-0469(1978)035<1536:REAACG>2.0.CO;2)
- Thompson, D. W. J., Bony, S., & Li, Y. (2017). Thermodynamic constraint on the depth of the global tropospheric circulation. *Proceedings of the National Academy of Sciences*, *114*(31), 8181–8186. <https://doi.org/10.1073/pnas.1620493114>
- Thompson, G., & Eidhammer, T. (2014). A study of aerosol impacts on clouds and precipitation development in a large winter cyclone. *Journal of the Atmospheric Sciences*, *71*(10), 3636–3658. <https://doi.org/10.1175/JAS-D-13-0305.1>
- Tippett, M. K., Lepore, C., Koshak, W. J., Chronis, T., & Vant-Hull, B. (2019). Performance of a simple reanalysis proxy for U.S. cloud-to-ground lightning. *International Journal of Climatology*, *39*(10), 3932–3946. <https://doi.org/10.1002/joc.6049>
- Virts, K. S., Wallace, J. M., Hutchins, M. L., & Holzworth, R. H. (2013). Highlights of a new ground-based, hourly global lightning climatology. *Bulletin of the American Meteorological Society*, *94*(9), 1381–1391. <https://doi.org/10.1175/BAMS-D-12-00082.1>
- Wacker, R. S., & Orville, R. E. (1999). Changes in measured lightning flash count and return stroke peak current after the 1994 U.S. National Lightning Detection Network upgrade: 1. Observations. *Journal of Geophysical Research*, *104*(D2), 2151–2157. <https://doi.org/10.1029/1998JD200060>
- Williams, E. R., Zhang, R., & Rydock, J. (1991). Mixed-phase microphysics and cloud electrification. *Journal of the Atmospheric Sciences*, *48*(19), 2195–2203. [https://doi.org/10.1175/1520-0469\(1991\)048<2195:MPMACE>2.0.CO;2](https://doi.org/10.1175/1520-0469(1991)048<2195:MPMACE>2.0.CO;2)
- Zipser, E., & Lutz, K. (1994). The vertical profile of radar reflectivity of convective cells: A strong indicator of storm intensity and lightning probability? *Monthly Weather Review*, *122*(8), 1751–1759. [https://doi.org/10.1175/1520-0493\(1994\)122<1751:TVPORR>2.0.CO;2](https://doi.org/10.1175/1520-0493(1994)122<1751:TVPORR>2.0.CO;2)
- Zipser, E. J. (1994). Deep cumulonimbus cloud systems in the tropics with and without lightning. *Monthly Weather Review*, *122*(8), 1837–1851. [https://doi.org/10.1175/1520-0493\(1994\)122<1837:DCCSIT>2.0.CO;2](https://doi.org/10.1175/1520-0493(1994)122<1837:DCCSIT>2.0.CO;2)